

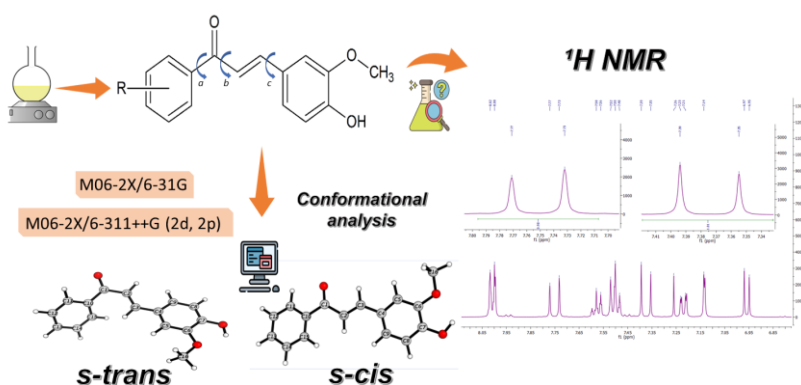
Full Paper | <http://dx.doi.org/10.17807/orbital.v17i2.21050>

Conformational Study, Synthesis, and Characterization of Chalcones Using 4-Hydroxy-3-methoxybenzaldehyde

Raphaela Pereira Guaringue* ^a, Vinícius Monteiro Schaffka ^a, Magno Roger Antonichen ^a, Thiago de Castro Rozada ^b, and Barbara Celânia Fiorin ^a

In this study, three chalcones derived from vanillin were synthesized and characterized: 4-hydroxy-3-methoxychalcone (Chal 1), 2',4-dihydroxy-3-methoxy-5'-nitrochalcone (Chal 2), and 4'-nitro-4-hydroxy-3-methoxychalcone (Chal 3), due to their documented biological importance, including antitumor and antioxidant activities. Acid-mediated aldol condensation was employed for synthesis, followed by characterization via NMR spectroscopy. Additionally, conformational analyses were performed using theoretical calculations with GAUSSIAN 09 software, identifying the *s-cis* conformation as predominant for all chalcones, with NBO calculations indicating hyperconjugative interactions that confer stability to this conformation relative to the evaluated compounds. These results expand the understanding of the structure-activity relationship of these chalcones, highlighting their potential for future pharmacological applications.

Graphical abstract



Keywords

Chalcone
Conformational analysis
DFT
NBO
NMR
Vanillin

Article history

Received 01 May 2024
Revised 13 Dec 2024
Accepted 20 Dec 2024
Available online 19 May 2025

Handling Editor: Sergio R. Lazaro

1. Introduction

Chalcones play a role as biosynthetic precursors of flavonoids. A distinctive characteristic of these compounds when present in nature is their yellow color, which, in basic medium, transforms into red [1]. Besides their natural occurrence, chalcones can be synthesized in the laboratory through various routes, including the Claisen-Schmidt aldol condensation. This reaction involves the combination of an acetophenone derivative with a benzaldehyde derivative in the presence of a strong alkaline base. Another method employed

is the aldol condensation in acidic medium, where Lewis acids are used as catalysts instead of basic mediums [1, 2]. These synthetic processes provide a versatile approach for obtaining chalcones with potential applications in various areas of research and industry.

The choice of vanillin as a precursor aldehyde is associated with its chemical structure similar to curcumin (Figure 1), a pigment with well-documented anticancer and

^aDepartment of Chemistry, State University of Ponta Grossa (UEPG). Ponta Grossa, Paraná, Brazil. ^b Department of Chemistry, State University of Maringá (UEM), Maringá, Paraná, Brazil, Corresponding autor E-mail: raphaelaguaringue@outlook.com

antioxidant properties [3, 4].

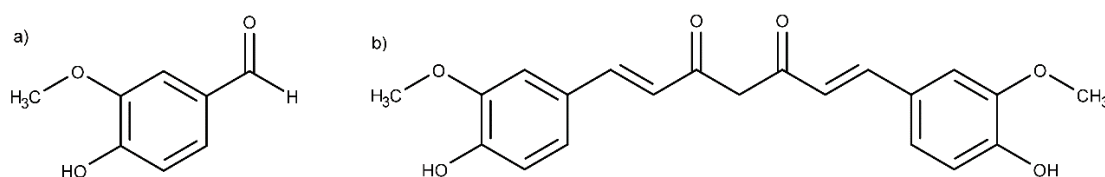


Fig. 1. Chemical structure of a) vanillin, b) curcumin.

The study aims to evaluate chalcones derived from vanillin, exploring the impact of different substituents on their chemical properties for subsequent biological application. There is a need to investigate how different substituents affect the biological behavior of chalcones. Thus, we proposed a conformational analysis of the chalcones under study, aiming to understand the stereo-electronic effects involved in their conformational equilibrium. This study will contribute to advancing understanding of the structure-activity relationship of chalcones, enabling the development of compounds with promising pharmaceutical potential [5, 6].

2. Material and Methods

2.1 Synthesis

The chalcones were synthesized through the condensation of a benzaldehyde and an acetophenone. In all three reactions, the benzaldehyde employed was vanillin. The acetophenones used were as follows: acetophenone to obtain 4-hydroxy-3-methoxychalcone, Chal 1, 2'-hydroxy-5'-nitroacetophenone for the synthesis of 2',4'-dihydroxy-3-methoxy-5'-nitrochalcone, Chal 2, and 4'-nitroacetophenone for 4'-nitro-4-hydroxy-3-methoxychalcone, Chal 3 (Fig. 2).

General Procedure [7]: In a 50 mL round-bottom flask, 3 mmol of vanillin, 3 mmol of the corresponding acetophenone, and 20 mL of methanol were added. As a catalyst, 5 mL of a 10% aqueous solution of *p*-toluenesulfonic acid (w/v) was employed. The reaction mixture was stirred for 48 hours at room temperature and shielded from light. The obtained product was washed with 60 mL of saturated sodium bicarbonate solution and subsequently extracted with ethyl acetate (3x20 mL). The organic phase was dried over anhydrous sodium sulfate, filtered, and then rotary-evaporated.

For the obtained products, ^1H and ^{13}C NMR spectra were acquired on a Nuclear Magnetic Resonance Spectrometer - Bruker, AVANCE III. The samples were dissolved in CDCl_3 .

2.2 Theoretical Calculations

Conformational analysis was performed using the GAUSSIAN-09 program package [8] and the molecular

visualization program GAUSS-VIEW 5.0.8. Initially, the structures were subjected to potential energy surface calculations as a function of their dihedral angles, with the angles rotated in 36 steps of 10° . These calculations were carried out using the DFT M06-2X method and the 6-31G basis set, resulting in the lowest energy structures for each chalcone.

Following these results, optimization and frequency calculations were conducted using the M06-2X/6-311++G(2d,2p) level of theory to adjust the angles and confirm the most stable structures.

NBO 5.9 calculations [9] were also employed, based on the Natural Bond Orbital theory, to determine the orbital interactions of the structures, revealing the effects that stabilize each conformation of the chalcones and influence conformational equilibrium.

The analysis of the global descriptive parameters was carried out to find a relationship between the chemical reactivity of the molecules and the sensitivity to structural disturbance, according to the methodology of Nazifi and collaborators. Where the values obtained from HOMO and LUMO are taken into account, to calculate the EA and IP, and with these values we can obtain the properties of hardness (η), softness (S), electronic chemical potential (μ) and electrophilic index (Ω) based on Koopman's theorem [10].

3. Results and Discussion

3.1 Synthesis

The synthesized chalcones are depicted in Fig. 2 and were characterized by ^1H NMR, confirming their obtainment. In the spectrum of Chal 1 (Fig. S1), all signals attributable to the chalcone of interest were clearly identified. The peaks observed in the range of 7.0 to 8.4 ppm correspond to the hydrogen atoms present in the aromatic rings and vinyl linkages. Two distinct doublets are noteworthy, located at 7.75 (H_α) and 7.37 ppm (H_β), respectively (Fig. 2). These signals resulting from the formation of the $\alpha\beta$ -unsaturation during the aldol condensation. Both exhibit a coupling constant ($^3J_{HH}$) of 15.6 Hz, indicative of the trans configuration of the hydrogen atoms in the vinyl linkage.

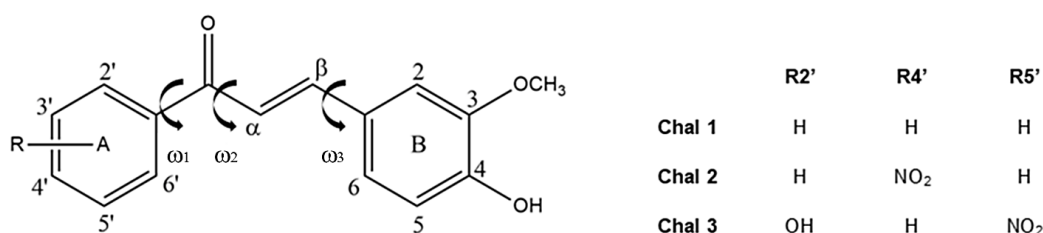


Fig. 2. Chalcones derived from vanillin.

The ^1H NMR spectra of Chal 2 and Chal 3 (Fig. S2 and S5) were evaluated, and for Chal 2, two-dimensional NMR (HSQC and HMBC) spectroscopy was conducted (Fig. S3 and S4), confirming the formation of the chalcones of interest.

(*E*)-1-(3-metoxi-4-hidroxifenil)-3-fenilprop-2-en-1-ona

(Chal 1): Yield: 52%; yellow solid; ^1H NMR (400 MHz, chloroform- d_4): δ = 8.02-8.00 (m, 2 H), 7.77-7.73 (d, J = 15.6 Hz, 1 H), 7.58-7.48 (m, 3 H), 7.39-7.35 (d, J = 15.6 Hz, 1 H), 7.23-7.21 (m, 1 H), 7.14 (s, 1 H), 6.97-6.95 (d, 1 H), 5.96 (s, 1 H), 3.96 (s, 3 H).

(*E*)-1-(4-hidroxi-3-metoxifenil)-3-(4-nitrofenil)prop-2-en-1-ona (Chal 2): Yield: 74%; yellow solid; ^1H NMR (400 MHz, chloroform- d_4): δ = 8.36-8.34 (d, 2 H), 8.14-8.12 (d, 2 H), 7.80-7.76 (d, J = 15.6 Hz, 1 H), 7.34-7.30 (d, J = 15.6 Hz, 1 H), 7.26-7.23 (m, 1 H), 7.14 (s, 1 H), 6.99-6.97 (d, 1 H), 6.00 (s, 1 H), 3.98 (s, 3 H).

(*E*)-1-(4-hidroxi-3-metoxifenil)-3-(2-hidroxi-5-nitrofenil)prop-2-en-1-ona (Chal 3): Yield: 46%; brown solid; ^1H NMR (400 MHz, chloroform- d_4): δ = 8.72-8.71 (d, 1 H), 8.39-8.35 (m, 1 H), 8.03-7.99 (d, J = 15.2 Hz, 1 H), 7.49-7.44 (d, J = 15.2 Hz, 1 H), 7.33-7.31 (dd, 1 H), 7.14-6.98 (m, 3 H), 4.04 (s, 3 H).

3.2 Theoretical Calculation

Conformational analysis was performed, starting with the initial rotation of angle α ($\text{C6}'\text{-C1}'\text{-C-O}$) (Fig. 2), resulting in the identification of energy minima. From these minimum energy conformations, rotations of angles b and c were conducted, resulting in the identification of six distinct conformations in total for Chal 1, six for Chal 2, and eight for Chal 3. Subsequently, optimization and frequency calculations were carried out on the structures obtained during the scanning process. The optimization step is crucial as it converges the structures to the lowest-energy geometries on the potential energy surface. Frequency calculations take into account molecular vibrations, refining the zero-point energy and adjusting angles to achieve conformations closer to reality. As a result, three minimum energy conformations were identified among the six studied for Chal 1 (Fig. 3), while the remaining structures converged to the same optimized structures. For Chal 2 and 3, four lowest energy structures were found for each, as evidenced in Figures 4 and 5, respectively. For both molecules, the most stable conformations with the highest population were those with *s-cis* configuration relative to the carbonyl and double bond. These molecules exhibit greater planarity compared to those with *s-trans* configuration.

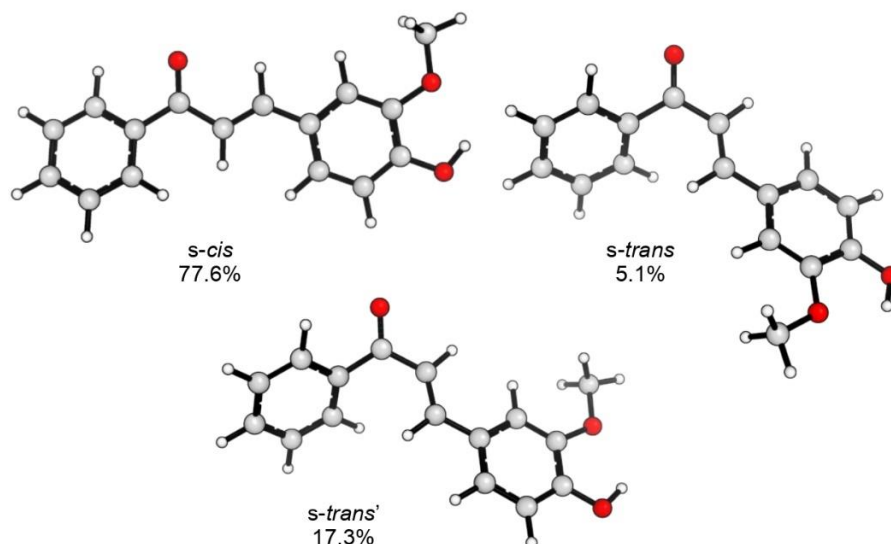


Fig. 3. Most stable geometries of Chal 1 obtained from optimization and frequency calculate at M06-2X/6-311++G (2d, 2p) level of theory.

To confirm and understand the stability of the found geometries, Natural Bond Orbital (NBO) calculations were performed (Table 1), which assess stabilization orbital

interactions and their respective energies, summing up the main stabilization energies of each previously obtained conformer.

Table 1. Main hyperconjugative interactions of Chal 1, Chal 2, and Chal 3 and their stabilization energies in kcal/mol, calculate at M06-2X/6-311++G (2d, 2p) level of theory.

| Orbital Interaction | Chal 1 | | | | Chal 2 | | | | Chal 3 | | | |
|--|----------------|--------------|-----------------|--------------|---------------|----------------|-----------------|--------------|---------------|----------------|----------------|--|
| | <i>s-trans</i> | <i>s-cis</i> | <i>s-trans'</i> | <i>s-cis</i> | <i>s-cis'</i> | <i>s-trans</i> | <i>s-trans'</i> | <i>s-cis</i> | <i>s-cis'</i> | <i>s-cis''</i> | <i>s-trans</i> | |
| π Ring B $\rightarrow \pi^*$ C=C | 26.36 | 31.61 | 31.65 | 33.93 | 28.55 | 32.63 | 27.26 | 29.45 | 35.01 | 26.72 | 29.30 | |
| π C=C $\rightarrow \pi^*$ C=O | 26.20 | 28.25 | 26.89 | 30.13 | 29.95 | 29.08 | 27.92 | 33.77 | 34.03 | .5.35 | 28.82 | |
| π Ring A $\rightarrow \pi^*$ C=O | 17.53 | 23.20 | 17.22 | 20.15 | 20.67 | 14.77 | 15.12 | 33.47 | 33.04 | 28.94 | 20.75 | |
| Ring A | 110.80 | 168.12 | 169.87 | 169.61 | 169.34 | 170.66 | 170.80 | 253.33 | 252.31 | 183.46 | 184.27 | |
| Ring B | 159.99 | 171.51 | 154.34 | 154.56 | 160.89 | 154.24 | 159.93 | 160.95 | 154.36 | 160.35 | 160.67 | |
| π Ring A $\rightarrow \pi^*$ NO ₂ | - | - | - | 31.77 | 31.76 | 28.24 | 28.27 | 62.80 | 62.55 | 35.97 | 48.33 | |
| LP _{C=O} | 45.68 | 47.48 | 45.38 | 51.44 | 51.23 | 49.56 | 49.54 | 19.29 | 19.17 | 19.25 | 19.45 | |
| LP _{NO2} | - | - | - | 318.95 | 319.71 | 319.59 | 319.37 | 44.36 | 45.31 | 44.56 | 44.48 | |
| LP _{OCH3} | 44.08 | 39.53 | 44.76 | 60.17 | 59.36 | 60.32 | 59.48 | 79.47 | 78.73 | 79.36 | 80.14 | |
| LP _{OH} | 41.09 | 33.07 | 35.28 | 42.83 | 42.01 | 42.80 | 41.89 | 124.25 | 125.52 | 82.99 | 71.85 | |
| TOTAL | 471.73 | 542.77 | 525.39 | 913.54 | 913.47 | 901.89 | 899.58 | 841.14 | 840.03 | 666.95 | 688.06 | |

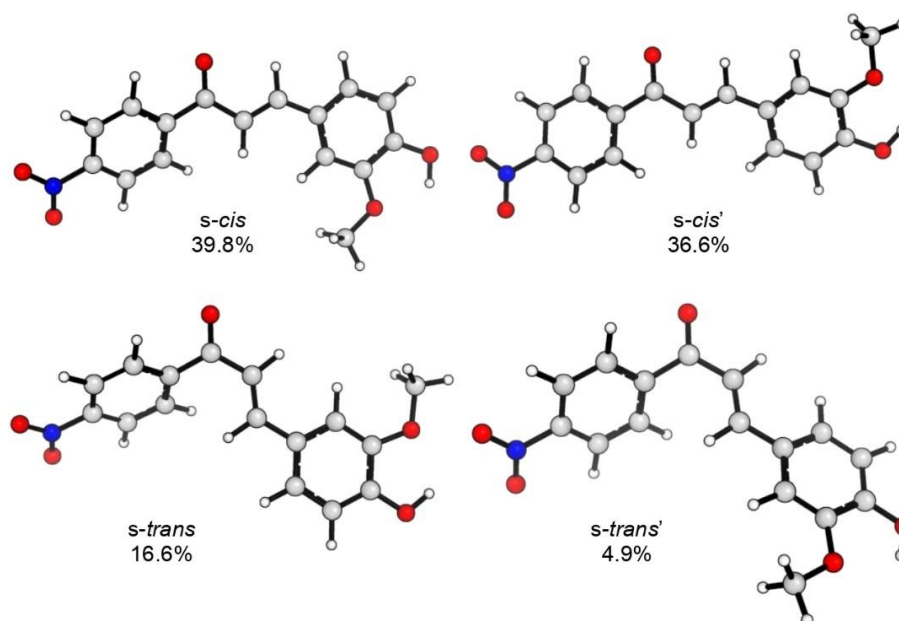


Fig. 4. Most stable geometries of Chal 2 obtained from optimization and frequency calculate at M06-2X/6-311++G (2d, 2p) level of theory.

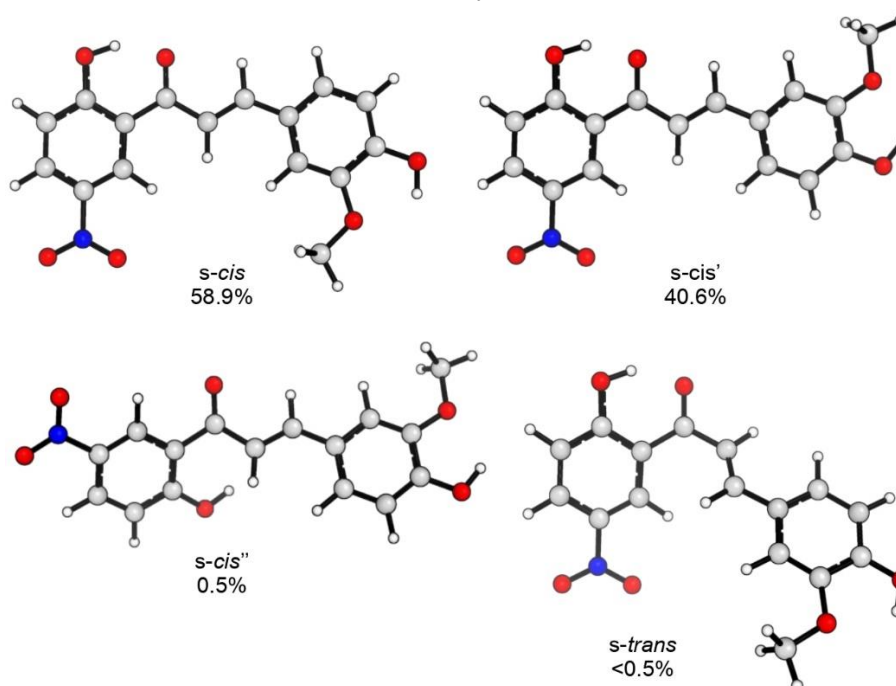


Fig. 5. Most stable geometries of Chal 3 obtained from optimization and frequency calculate at M06-2X/6-311++G (2d, 2p) level of theory.

For Chal 1, it can be observed that the greatest energy difference between the most stable conformers lies in the stabilization of aromatic B with its substituents and the carbonyl with aromatic A, with the carbonyl orbital acting as an acceptor and the aromatic A as a donor of electronic density in their orbitals. The planarity of the *s-cis* conformation brings about the most effective hyperconjugative effect in this molecule, without presenting steric effects. The dihedral angle influences the overlap of orbitals and consequently the stabilization energy (Table S1). We can observe that the *s-cis* conformers show less deviation from the angles of 0 and 180 degrees (ideal angles). The planarity of the molecule facilitates the overlap of π orbitals, thereby increasing electronic conjugation within the structure. This can stabilize the molecule as energy is more easily

delocalized among the atoms of the π system, resulting in a more uniform distribution of electronic density [6].

Among the lowest energy conformers of Chal 2, the greatest energy difference observed lies in the interaction between the carbonyl and aromatic A. This occurs due to the variation of the dihedral angle in the corresponding structures, which does not favor the donation of electronic density between the donor and acceptor orbitals in the *s-trans* conformations, as electron delocalization is hindered. Thus, angles closer to 0° and 180° are more favorable.

For Chal 3, it can be observed that the stabilization energies of the *s-cis* and *s-cis'* conformations are higher compared to the energies of the *s-cis''* and *s-trans* conformations. This is due to the energy of aromatic A, which shows significant differences, being higher for the *s-cis* and *s-*

cis' conformers.

It was possible to identify the most stable conformations of each studied chalcone, observing the predominance of the population of *s-cis* conformers. This indicates greater stability of planar structures, as interactions between the $\pi \rightarrow \pi^*$ orbitals are favored in this conformational arrangement. In the *s-trans* conformation, bulky groups attached to the carbon atoms adjacent to the double bond may experience steric strain, leading to a tendency for molecular twisting to relieve these strains. This twisting reduces the planarity of the molecule. These $\pi \rightarrow \pi^*$ interactions are important for structural stability and can significantly influence the physical and chemical properties of chalcone molecules, including their biological activities and potential applications in various scientific and industrial fields [6].

In some cases, the presence of substituents can increase the stability of the chalcone, especially if these substituents contribute to enhancing electronic resonance or stabilizing

the planar conformation of the molecule. We noticed that this occurs when comparing Chal 1. On the other hand, certain bulky substituents may prevent the attainment of a planar conformation and thus decrease the stability of the chalcone. Additionally, some substituents may introduce unfavorable steric interactions that impair the stability of the molecule [6]. Some studies suggest the importance of this planar geometry for biological activity, directly affecting its ability to interact with specific targets, as it affects reactivity. Electron withdrawing or donor substituents also interfere with the molecule's reactivity, modulating biological activity [12].

To understand the reactivity of the compounds based on their energies HOMO and LUMO the boundary orbital analysis was performed. Structures with higher HOMO energy are better electron donors. As shown in Table 2, Chal 1 obtained the highest value. The molecule with the lowest energy LUMO is the best electron acceptor, Chal 2 presented the lowest value.

Table 2. Calculated values for the frontier orbitals (E_{gap} , EA, IP) and properties of hardness (η), softness (S), electronic chemical potential (μ) and electrophilic index (Ω) in eV. Calculate at M06-2X/6-311++G (2d, 2p)

| Compound | HOMO | LUMO | E_{gap} | EA | IP | h | S | m | W |
|----------|-------|-------|------------------|------|------|------|--------|-------|------|
| Chal 1 | -7.22 | -1.39 | 5.82 | 1.39 | 7.22 | 2.91 | 127.22 | -4.31 | 3.19 |
| Chal 2 | -7.47 | -2.16 | 5.31 | 2.16 | 7.47 | 2.65 | 139.40 | -4.82 | 4.97 |
| Chal 3 | -7.58 | -2.06 | 5.51 | 2.06 | 7.58 | 2.75 | 134.14 | -4.82 | 4.21 |

Another parameter analyzed is the E_{gap} , the lower, the greater the reactivity of the molecule. This is because a smaller energy difference facilitates the transition of electrons from the HOMO orbital to the LUMO, which may indicate that the molecule is more likely to participate in chemical reactions, such as electron donation or acceptance [13]. It may be related to the better antioxidant activity of the compound, since it has a greater capacity to neutralize free radicals, the lowest value was for Chal 2, followed by Chal 1 and Chal 3. Zainuri, et al. described that the nitro group brings this decrease in the E_{gap} of the molecule because it is a strongly electron-stripping group, causing it to stabilize the HOMO and LUMO orbitals, resulting in a smaller energy difference between them [11].

Electron affinity (EA) and ionization potential (IP) also indicate the antioxidant potential of the molecules. Since the higher the EA value, the easier it is to remove an electron from a compound. And for IP, a high value indicates a lower tendency to electron donation, so the lower the IP, the better the ability to remove the electron in the HOMO orbital from the neutral form of the antioxidant molecule. Chal 2 showed the greatest potential to accept electrons from a free radical, as it had the highest EA. Chal 1 presented the lowest IP value, which makes it a promising electron donor for free radicals, these values are in agreement with the values of HOMO and LUMO [10].

Polarizability is related to the size of the atoms and the ease of distortion of their electron cloud, being greater in larger atoms and ions. It connects directly to molecular softness (S), as more polarizable molecules are smoother and more reactive. In contrast, the hardness (h), which is approximately half the E_{gap} between the HOMO and LUMO energies, reflects the molecule's resistance to electronic changes. Molecules with smaller HOMO-LUMO gaps, softer and more polarizable, tend to be more reactive, while harder molecules are less reactive and less polarizable [13]. The values of hardness (h) and softness (S) are complementary and indicate the reactivity of the molecule in the face of changes in electron density. For both, the most reactive

molecule studied was Chal 2, this occurs due to the presence of the electron-removing nitro group, which decreases the molecules E_{gap} , making it less stable.

The electronic chemical potential (m) describes the tendency of a molecule to lose and gain electrons, it is related to its electronegativity. Negative values mean that the molecule tends to be an electron acceptor, both chalcones studied showed negative values, the highest value was for Chal 1. The electrophilicity index (Ω) is calculated from m and h, indicating the ability of a molecule to accept electrons in a reaction, so Chal 2 presented the highest value being the most electrophilic molecule. [10].

4. Conclusions

From the characterization by ^1H NMR, it was possible to confirm the formation of the chalcones of interest using the acid-mediated synthesis method. Through conformational analysis, the most stable conformations of each chalcone were identified, with a predominant population of *s-cis* conformers observed, indicating greater stability of planar structures due to favored interactions of the $\pi \rightarrow \pi^*$ orbitals. Therefore, the stability of a chalcone depends on the contribution of all substituents present in the molecule and how they interact to influence its structure and conformational energy. Chal 2 was the most reactive and electrophilic molecule among the others studied. The presence of the nitro group decreases the E_{gap} increasing its reactivity, increases its acceptance of electrons. The lower hardness value reinforces its high reactivity, this characteristic suggests a better ability to neutralize free radicals, and may be a promising molecule in terms of antioxidant potential and reactivity.

Acknowledgments

The authors thank the CAPES for fellowship, the C-LABMU and University of Ponta Grossa (UEPG) for the research facilities.

Supporting Information

NMR spectra (1D and 2D) of the synthesized compounds and Table with relative energies (in kcal/mol) and dihedral angles of the conformers of Chal 1, Chal 2, and Chal 3.).

Author Contributions

Both BC Fiorin and TC Rozada contributed in conceptualization, project administration, supervision and writing. RP Guaringue especially was responsible for formal analysis and writing. MR Antonichen contributed in writing, VM Schaffka Was responsible for data analysis and discussion.

References and Notes

- [1] Rajendran, G.; Bhanu, D.; Aruchamy, B.; Ramani, P.; Pandurangan, N.; Bobba, K. N.; Oh, E. J.; Chung, H. Y.; Gangadaran, P.; Ahn, B. C. *Pharmaceuticals* **2022**, *15*, 1250. [\[Crossref\]](#)
- [2] Nadia, A. A.; Elkanzi, H. H.; Ruba, A.; Alolayan, W. D.; Fatin, M. Z.; Rania, B. B. *ACS Omega* **2022**, *7*, 27769. [\[Crossref\]](#)
- [3] Raghavan, S.; Manogaran, P.; Kuppuswami, B. K.; Venkatraman, G.; Kumari, K.; Narasimha, G. *Med. Chem. Res.* **2015**, *24*, 4157. [\[Crossref\]](#)
- [4] Weber, W. M.; Hunsaker, L. A.; Abcouwer, S. F.; Deck, L. M.; Vander Lagt, D. L. *Bioorg. Med. Chem.* **2005**, *13*, 3811. [\[Crossref\]](#)
- [5] Kerek, A. L.; Rozada, T. de C.; Fiorin, B. C. *Orbital: Electron. J. Chem.* **2021**, *13*, 120. [\[Crossref\]](#)
- [6] Emiliano, H. V.; Guaringue, R. P.; Rozada, T. de C.; Fiorin, B. C. *Orbital: Electron. J. Chem.* **2021**, *13*, 182. [\[Crossref\]](#)
- [7] Kim, J. H.; Ryu, H. W.; Shim, J. H.; Park, K. H.; Withers, S.G. *Chembiochem.* **2009**, *10*, 2475. [\[Crossref\]](#)
- [8] Frisch, M. J. et al., Gaussian-09, Revision A.01, Gaussian Inc, Wallingford, CT. **2009**.
- [9] Glendening, E. D.; Badenhoop, J. K.; Reed, A. E.; Carpenter, J. E.; Bohmann, J. A.; Morales, C. M.; Weinhold, F. **2009**. NBO 5.9. Theoretical Chemistry Institute, University of Wisconsin, Madison, WI.
- [10] Nazifi, S. M. R.; Asgharshamsi, M. H.; Dehkordi, M. M.; Zborowski, K. K. *Free Radic. Res.* **2019**, *53*, 922. [\[Crossref\]](#)
- [11] Zainuri, D. A.; Alsaee, S. K.; Zaini, M. F.; Ab Rahman, S. N. F.; Bakar, M. A. A.; Abdullah, M.; Razak, I. A.; Arshad, S. *Physica B: Condensed Matter.* **2023**, *655*, 414744. [\[Crossref\]](#)
- [12] Marquina, S.; Maldonado-Santiago, M.; Sánchez-Carranza, J. N.; Antúnez-Mojica, M.; González-Maya, L.; Razo-Hernández, R. S.; Alvarez, L. *Bioorg. Med. Chem.* **2019**, *27*, 43. [\[Crossref\]](#)
- [13] Carey, F. A. *Advanced Organic Chemistry, Part A*. 4. ed. New York: Wiley, 1937.

How to cite this article

Guaringue, R. P.; Schaffka, V. M.; Antonichen, M. R.; Rozada, T. C.; Fiorin, B. C. *Orbital: Electronic J. Chem.* **2025**, *17*, xx. DOI: <http://dx.doi.org/10.17807/orbital.v17i2,21050>